

Kelvin waves cascade in superfluid turbulence

D. Kivotides¹, J.C. Vassilicos², D.C. Samuels¹ and C.F. Barenghi^{3,1}

¹*Mathematics Department, University of Newcastle, Newcastle NE1 7RU, UK,*

²*DAMTP, University of Cambridge, Cambridge CB3 9EH, UK,*

³*Newton Institute, University of Cambridge, Cambridge CB3 0EH, UK*

(November 16, 2000)

Abstract

We study numerically the interaction of four initial superfluid vortex rings in the absence of any dissipation or friction. We find evidence for a cascade of Kelvin waves generated by individual vortex reconnection events. The Kelvin wave cascade transfers energy to higher and higher wavenumbers k . After the vortex reconnections occur the energy spectrum scales like k^{-1} and the curvature spectrum becomes flat. These effects highlight the importance of Kelvin waves and reconnections in the transfer of energy within a turbulent vortex tangle.

PACS 67.40Vs, 47.37.+q

Typeset using REVTeX

When studying a physical system which is dynamically complex, an important issue to consider is the effect of nonlinearity on the distribution of energy over the degrees of freedom of the system. For example, it is well known that in the case of a classical viscous flow the nonlinear terms of the Navier-Stokes equation redistribute the energy over various scales of motion without affecting the total energy budget. In this case the celebrated Richardson cascade of eddies leads to Kolmogorov's $k^{-5/3}$ dependence of energy on wavenumber k . The aim of our letter is to describe a form of energy cascade of helical waves on vortex filaments (Kelvin waves). Our argument is that vortex reconnections leave behind regions of high curvature which generate Kelvin waves (oscillations of a filament's position). Nonlinear interactions between the Kelvin waves transfer energy to higher Kelvin wavenumbers k' . We use the term 'Kelvin wavenumber' to distinguish between this wavenumber k' (the wavenumber along the vortex filament) and the magnitude $k = |\mathbf{k}|$ of the wavevector \mathbf{k} of the Fourier spectrum of three-dimensional space x, y, z . We investigate the Kelvin wave cascade process through direct numerical simulations of vortex filament dynamics and show that this wave cascade is clearly visible in the spectra of vortex line curvature, torsion, and line velocity.

Although our system is classical (essentially, it consists of vortex filaments governed by the inviscid, incompressible Euler equation) the motivation behind our work is the desire to understand the turbulent state of superfluid He II. This form of turbulence, which takes the form of a tangle of vortex filaments, is currently attracting experimental [1] [2] [3] [4] [5] and theoretical attention [6] [7] [8] [9] [10] [11]. A superfluid vortex filament has two key properties [12]: the first is the microscopic size of the vortex core radius, $a \approx 10^{-8}$ cm; the second is the quantization of the circulation, which takes a fixed value $\Gamma = 9.97 \times 10^{-4}$ cm²/sec given by the ratio of Planck's constant and the mass of a helium atom. The smallness of a , the fact that the values of the core size and the circulation are the same for all filaments, and finally the superfluid's lack of viscosity, are all ingredients for which it is natural to use the classical theory of vortex filaments [13] to describe the dynamics of the superfluid turbulence. Therefore we represent a vortex filament as a curve $\mathbf{s} = \mathbf{s}(\xi, t)$ in three dimensional space (where ξ is arclength and t is time) [14]. At each position \mathbf{s} along

a filament we also define the three right handed unit vectors $\hat{\mathbf{t}}$, $\hat{\mathbf{n}}$ and $\hat{\mathbf{b}}$ along the tangent, normal and binormal directions respectively. We also define the local curvature $c(\xi) = |\mathbf{s}''|$ and torsion $\tau(\xi) = |\hat{\mathbf{b}}'|$, where a prime denotes derivative with respect to arclength. The curve moves with velocity \mathbf{v}_L at the point \mathbf{s} given by the Biot-Savart law

$$\mathbf{v}_L = \frac{d\mathbf{s}}{dt} = \frac{\Gamma}{4\pi} \int \frac{(\mathbf{r} - \mathbf{s}) \times d\mathbf{r}}{|\mathbf{r} - \mathbf{s}|^3}. \quad (1)$$

In writing (1) we neglect the friction against the normal fluid component, that is to say we concentrate our attention to the low temperature turbulence studied experimentally by McClintock and coworkers [2] and theoretically by Tsubota [7]. In order to calculate numerically [15] the time evolution of a configuration of vortices we use the Biot - Savart law (1) together with the assumption that vortex filaments reconnect when they approach each other at sufficiently short distance. This extra assumption is justified by results obtained [16] using the more microscopic Bose- Einstein condensate model which describes phenomena (such as reconnections) which happen on the quantum mechanical healing length scale of the vortex core a . Our numerical method will be described with more details elsewhere [17]; here it suffices to say that the filaments are discretized with a variable number of mesh points (the calculation reported in the figures have 576 points at $t = 0\text{sec}$ and 927 points at $t = 0.129\text{sec}$) and that the time step Δt is also variable, but typically it has value $\Delta t \approx 0.0008\text{sec}$.

Our numerical calculation begins with four superfluid vortex rings of radius 0.023cm placed on the opposite sides of a cube of size 0.0639cm (see the first picture in Figure 1) and oriented so that they all move toward the center of the cube [18]. This vortex configuration is convenient for our purpose because, unlike other more complex configurations [7] [10], it is simple enough to investigate the effects of an individual reconnection. Figure 1 shows four snapshots during the time evolution. The four rings approach each other and undergo four symmetric reconnections at time $t_c = 0.059\text{sec}$. Each reconnection introduces a cusp which then relaxes, generating large amplitude Kelvin waves (see the third picture of Figure 1). As time proceeds, the vortex filaments assume a crinkled shape, which is apparent in the

last picture of Figure 1, because there is no friction with the normal fluid to smooth small scale waves. A similar effect has been seen by Tsubota [7] in recent simulations.

During the approach of the vortex rings to reconnection very little vortex wave is visible on the rings, even though the non-local Biot-Savart equation of vortex line motion is used. Since vortex lines approaching reconnection tend to twist to an antiparallel orientation, our initial conditions in which the vortices are approaching each other in an antiparallel manner may be preventing the generation of strong vortex waves before reconnection. If so, this is fortunate in that it allows us to study the behavior of the vortex waves radiating from the reconnection event itself, without the distraction of the Kelvin waves due to the reorientation motion of the filaments prior to reconnection.

Since our model is incompressible there is no loss of energy by the generation of sound either during the reconnection event itself or as an effect of the motion of the filaments [19]. In a real system however these processes must take place and they would represent dissipation processes even in the pure inviscid superfluid at absolute zero temperature. The loss of vortex energy to sound emission will be most effective [6] at high Kelvin wavenumbers $k' > k_{sound}$. We need therefore a mechanism to transfer energy to high Kelvin wavenumbers. We show in this letter that isolated (and rare) reconnection events along with the nonlinear transport of energy between wave modes provide this mechanism.

To study this energy transfer we first consider the spectrum $E_V(k)$ of the superfluid velocity field \mathbf{v}_s , hereafter referred to as the energy spectrum (or the spectrum of the Eulerian velocity) which is such that

$$\frac{\rho_s}{2} \int \int \int v_s^2(x, y, z) dx dy dz = \int_0^\infty E_V(k) dk. \quad (2)$$

where ρ_s is the superfluid density. The results of this calculation are shown in Figure 2. Isolated and straight vortex filaments have a $1/r$ velocity field, and thus have a k^{-1} energy spectrum. For our initial conditions of four large rings the energy spectrum shows approximately an exponential behaviour (see the two bottom curves of Figure 2). After

the reconnections occur and the reconnected vortex lines begin to move further apart, the energy spectrum develops approximately a k^{-1} form (see the two top curves of Figure 2). The energy spectrum in the high k region rises after the reconnections, directly illustrating the transfer of energy to high k values by the reconnection events. The energy spectrum after reconnection has the same k^{-1} form of the spectrum of an isolated vortex filament. This is a bit unfortunate since it is difficult to distinguish the exponential form and the k^{-1} form at intermediate values of k , so the shape of $E_V(k)$ is relatively unaffected by the cascade.

To study this energy transfer in more detail and confirm the Kelvin wave cascade, it is more instructive to consider the curvature spectrum which is such that

$$\frac{1}{2} \int c^2(\xi) d\xi = \int E_C(k') dk', \quad (3)$$

where the right-hand-side integral is taken over the Kelvin wavenumber k' .

This spectrum is initially a delta function (representing the curvature of the four rings) and it remains a sharp function until the time t_c of the reconnection event. Curvature spectra at different times $t > t_c$ are shown in Figure 3a,b,c. It is interesting to note that as soon as the reconnection takes place $E_C(k')$ becomes nonzero at all Kelvin wavenumbers, so, strictly speaking, two energy transfer mechanisms are operating: the instantaneous transfer of energy to a wide range of curvatures by the reconnection event and the following redistribution of that energy by nonlinear interactions. The effect of the reconnection is non-local in curvature space (meaning that it affects a wide range of curvatures simultaneously) while the nonlinear wave interactions are primarily local interactions, exchanging energy between neighboring wavelength scales [20].

If one gives enough time for the nonlinear interaction between the Kelvin waves to equilibrate in some statistical sense, one sees that the spectrum E_C becomes constant (Figure 3c). It takes some time to reach this equilibration, and during this equilibration process the plateau region of the spectrum spreads from low k' to high k' . This is a consequence of

the local nature of the Kelvin wave cascade. However, Figure 3 shows that it takes only a short time (only 0.03 seconds after the reconnection) to reach this equilibrium value over a significant range of the spectrum. This indicates that the nonlinear interaction of the Kelvin waves is not weak and cannot be ignored in theories of superfluid turbulence.

Why should the curvature spectrum $E_C(k')$ be constant? The parameters of the system are Γ , ρ_s , the characteristic vortex separation distance ℓ in a dense vortex tangle, and the rate of vortex energy dissipation ϵ_{sound} to sound emission at high Kelvin wavenumbers k_{sound} and above. If an equilibrium cascade of Kelvin waves is achieved [6] in the range $\ell^{-1} \ll k' \ll k_{sound}$ then we argue that the large and small scale parameters ℓ and ϵ_{sound} do not affect $E_C(k')$ in that range, hence $E_C(k') = E_C(\rho_s, \Gamma, k')$. The curvature spectrum $E_C(k')$ is dimensionless - see Equation (3) - and dimensional constraints imply that $E_C(k')$ must be independent of ρ_s , Γ and k' and be simply equal to a dimensionless constant in the range $\ell^{-1} \ll k' \ll k_{sound}$. Figure 3 confirms this argument. An identical dimensional argument can be made for the spectrum $E_T(k')$ of the torsion. The torsion spectrum is also equal to a dimensionless constant in the Kelvin wave cascade range of wavenumbers, and evidence for this is given in Figure 4.

The spectrum $E_L(k')$ of the (Lagrangian) velocity \mathbf{v}_L is such that

$$\frac{\rho_s}{2} \int v_L^2(\xi) d\xi = \int E_L(k') dk'. \quad (4)$$

Because $v_L \approx \Gamma c$ to the leading approximation [14], and because E_C does not depend on k' , neither does E_L , and in fact $E_L \sim \Gamma^2$. Furthermore, equation (4) implies that E_L is proportional to ρ_s , hence $E_L(k') \sim \rho_s \Gamma^2$. The only way to balance this equation dimensionally with the remaining parameters ℓ and ϵ_{sound} is to multiply the right hand side times ℓ^2 . We conclude that

$$E_L(k') \sim \ell^2 \rho_s \Gamma^2. \quad (5)$$

Figure 5 confirms that E_L does not depend on k' .

We now consider the energy spectrum $E_V(k)$. Vinen [6] introduced a "smoothed" length of vortex line per unit volume, obtained after all the Kelvin waves have been removed, and considered $E_K(k')dk'$, the energy per unit length of smoothed vortex line associated with Kelvin waves in the range k' to $k' + dk'$. By dimensional analysis he found that $E_K(k') \sim \rho_s \Gamma^2 k'^{-1}$. We notice that, because the fluctuations of the velocity field are induced by the Kelvin wave fluctuations on the filaments, it is reasonable to expect that $E_V(k) \sim E_K(k')$ with $k' \sim k$. Because the length of smoothed vortex lines scales with ℓ , we have $E_V(k) \sim \ell E_K(k')$. Using Vinen's result, we obtain $E_V \sim \ell \rho_s \Gamma^2 k^{-1}$, in agreement with the k^{-1} dependence observed after reconnections in Figure 2.

In conclusion we have found direct numerical evidence of the cascade process in the interaction of Kelvin waves directly after individual reconnection events on vortex filaments. The effect of this cascade on the spectra for curvature, vortex line velocity and torsion is strong. The computed spectra confirm our scaling arguments. These results highlight the importance of reconnections and Kelvin waves on the transfer of energy within a turbulent superfluid vortex tangle. This work should also stimulate more efforts in the development of micro-instrumentation: existing measurements of velocity spectra [5] cannot yet resolve the small scales under discussion here, due to the relative large size of the probes.

ACKNOWLEDGMENTS

This research is supported by the Leverhulme Trust. We thank the Isaac Newton Institute and DAMPT, Cambridge University, where part of this work was carried out. JCV is grateful for financial support from the Royal Society.

REFERENCES

- [1] M.R. Smith, R.J. Donnelly, N. Goldenfeld and W.F. Vinen, Phys. Rev. Lett. **71** 2583 (1993); S.R. Stalp, L. Skrbek and R.J. Donnelly, Phys. Rev. Lett. **82** 4381 (1999).
- [2] S.I. Davis, P.C. Hendry and P.V.E. McClintock, Physica B **280** 43 (2000).
- [3] M.R. Smith, D.K. Hilton and S.V. VanSciver, Phys. Fluids **11** 751 (1999).
- [4] M. Niemetz, W. Schoepe, J.T. Simola and J.T. Tuoriniemi, Physica B **280** 559 (2000).
- [5] J. Maurer and P. Tabeling, Europhys. Letters **43** 29 (1998).
- [6] W.F. Vinen, Phys. Rev. B **61** 1410 (2000).
- [7] M. Tsubota, T. Araki and S.K. Nemirowskii, J. Low Temp. Phys. **119** 337 (2000).
- [8] D.C. Samuels and D. Kivotides, Phys. Rev. Lett. **83** 5306 (1999).
- [9] O.C. Idowu, D. Kivotides, C.F. Barenghi and D.C. Samuels, J. Low Temp. Phys. **120** 269 (2000).
- [10] C. Nore, M. Abid and M.E. Brachet, Phys. Rev. Lett. **78** 3896 (1997).
- [11] B.V. Svistunov, Phys. Rev. B **52** 3647 (1995).
- [12] R.J. Donnelly, *Quantized vortices in helium II*, Cambridge University Press, Cambridge 1991.
- [13] P.G. Saffman, *Vortex dynamics*, Cambridge University Press, Cambridge 1992.
- [14] K.W. Schwarz, Phys. Rev. B **31** 5782 (1985).
- [15] D.C. Samuels Phys. Rev. B **46** 11714 (1992).
- [16] J. Koplik and H. Levine, Phys. Rev. Lett. **71** 1375 (1993).
- [17] O.C. Idowu, D. Kivotides, C.F. Barenghi and D.C. Samuels, to be published in *Quantized vortex dynamics and superfluid turbulence*, ed by C.F. Barenghi, R.J. Donnelly

and W.F. Vinen, Lecture Notes in Physics, Springer.

[18] M. Kiya and H. Ishii, Fluid Dynam. Res. **8** 73 (1991).

[19] M. Leadbeater, T. Winiecki, D.C. Samuels, C.F. Barengi and C.S. Adams, submitted.

[20] D.C. Samuels and R.J. Donnelly, Phys. Rev. Lett. **64** 1385 (1990).

FIGURES

FIG. 1. Vortex configurations at $t = 0.0\text{sec}$ (initial state), $t = 0.059\text{sec}$ (first reconnection), $t = 0.69\text{sec}$ (note the Kelvin waves) and $t = 0.129\text{sec}$ (note the crinkled shape of the filaments).

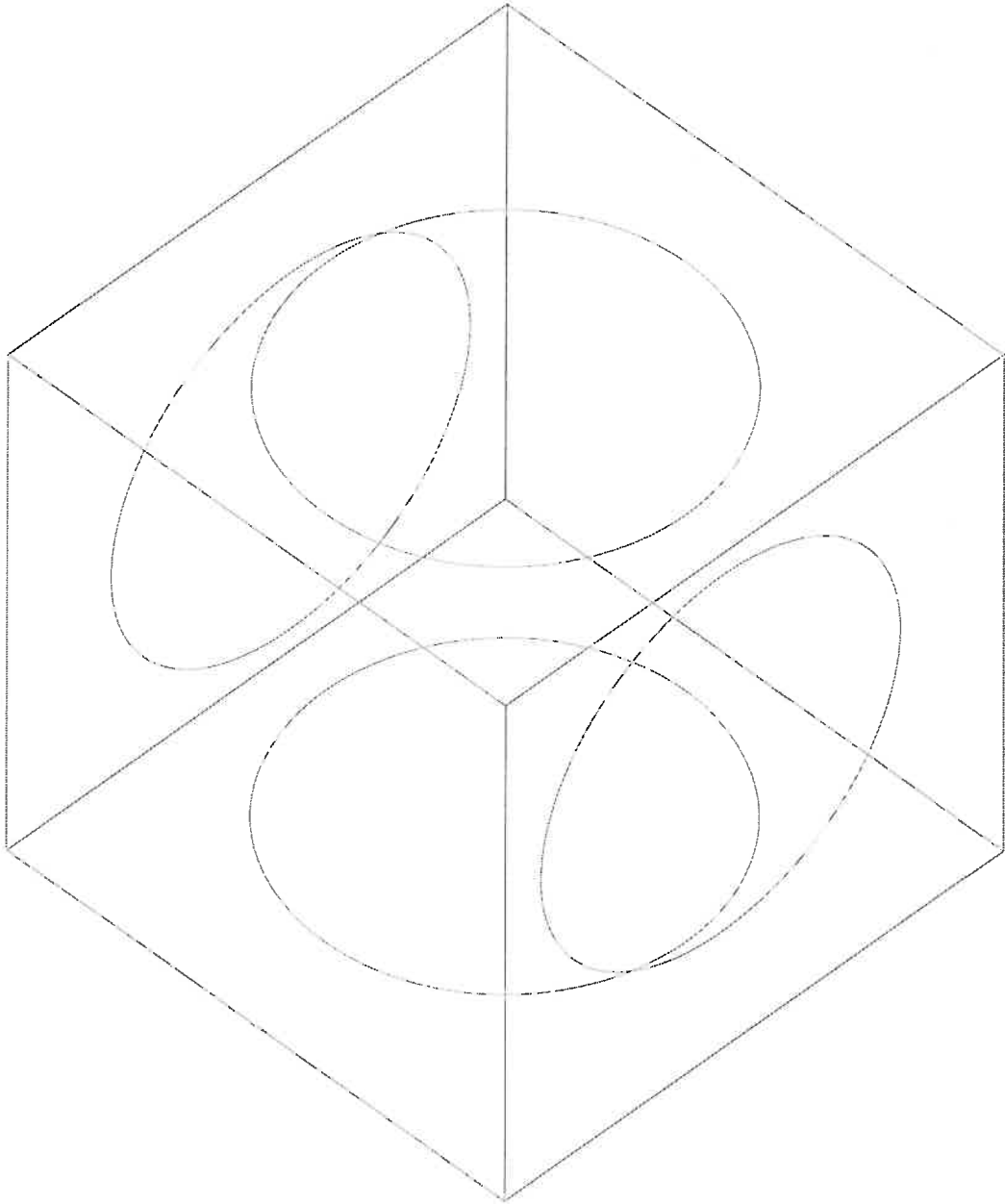
FIG. 2. Velocity spectra $E_V(k)$ before the reconnections (lower two curves at $t = 0.0\text{sec}$ and $t = 0.030\text{sec}$) and after the reconnections (upper two curves at $t = 0.069\text{sec}$ and $t = 0.089\text{sec}$). The spectra are obtained by discretizing the computational box into 64^3 mesh points.

FIG. 3. Curvature spectra $E_C(k')$ at (a) $t = 0.069\text{sec}$, (b) $t = 0.089\text{sec}$ and (c) $t = 0.109\text{sec}$.

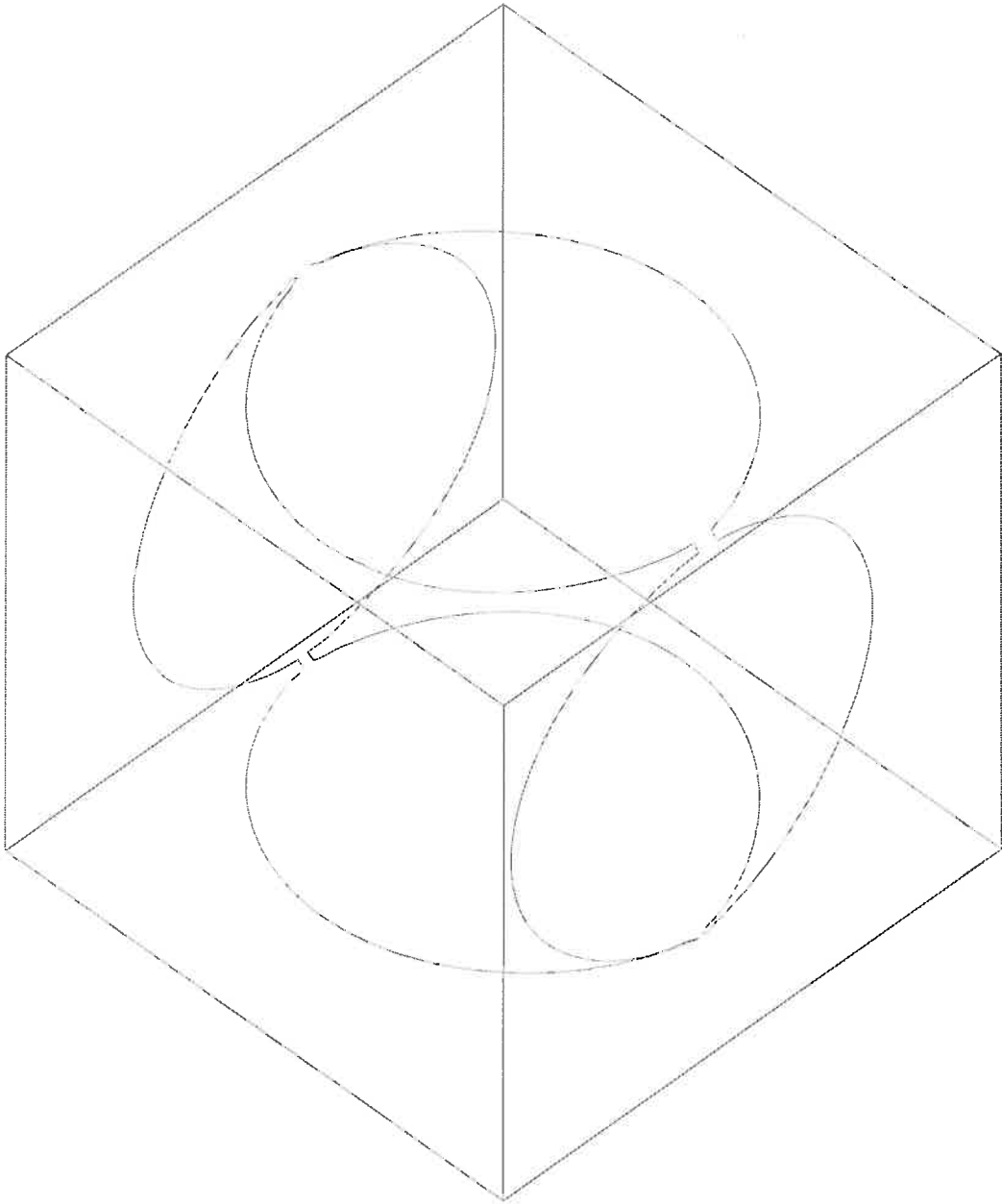
FIG. 4. Torsion spectrum $E_T(k')$ at $t = 0.109\text{sec}$.

FIG. 5. Lagrangian velocity spectrum $E_L(k')$ at $t = 0.109\text{sec}$.

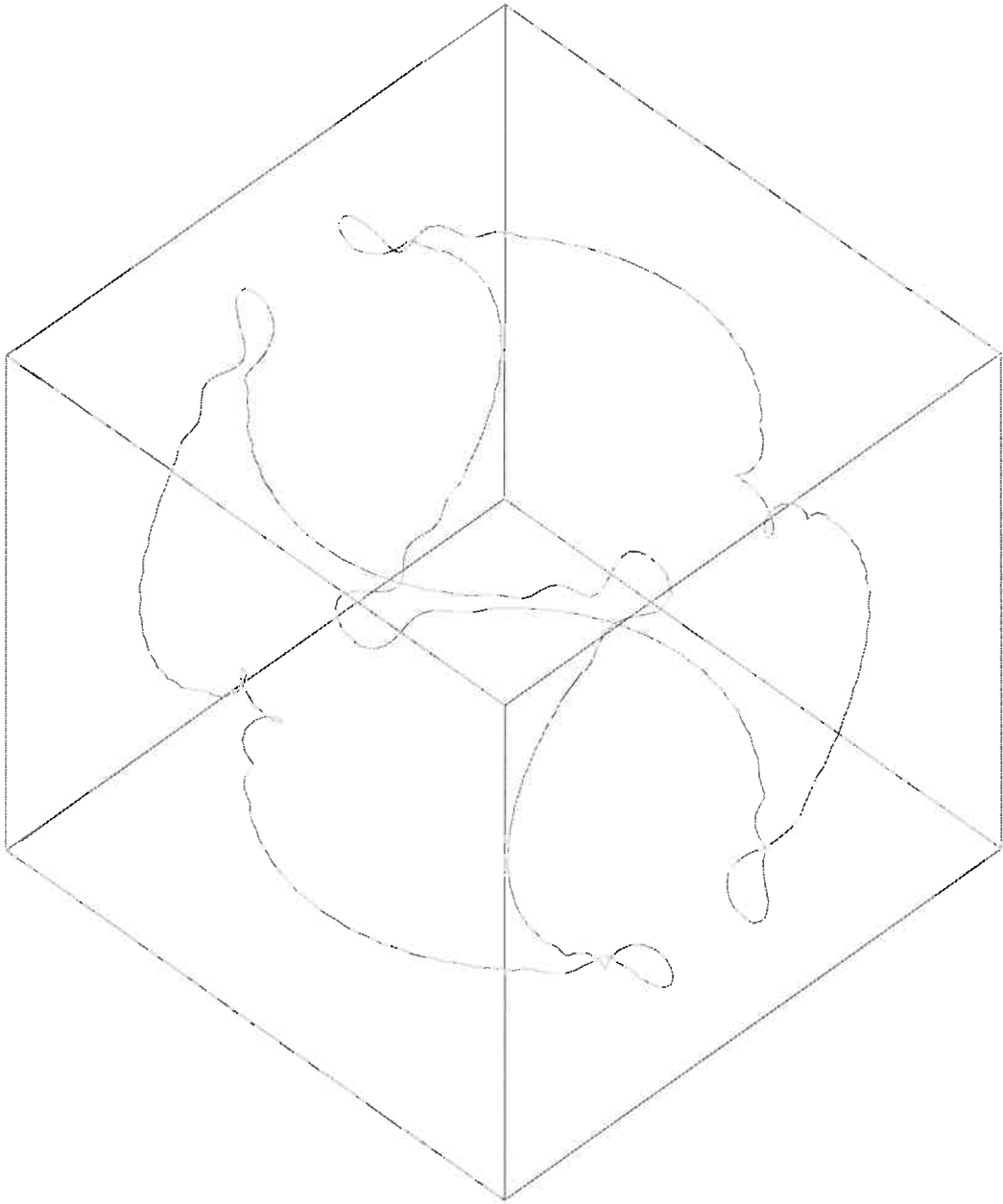
$t=0.000$



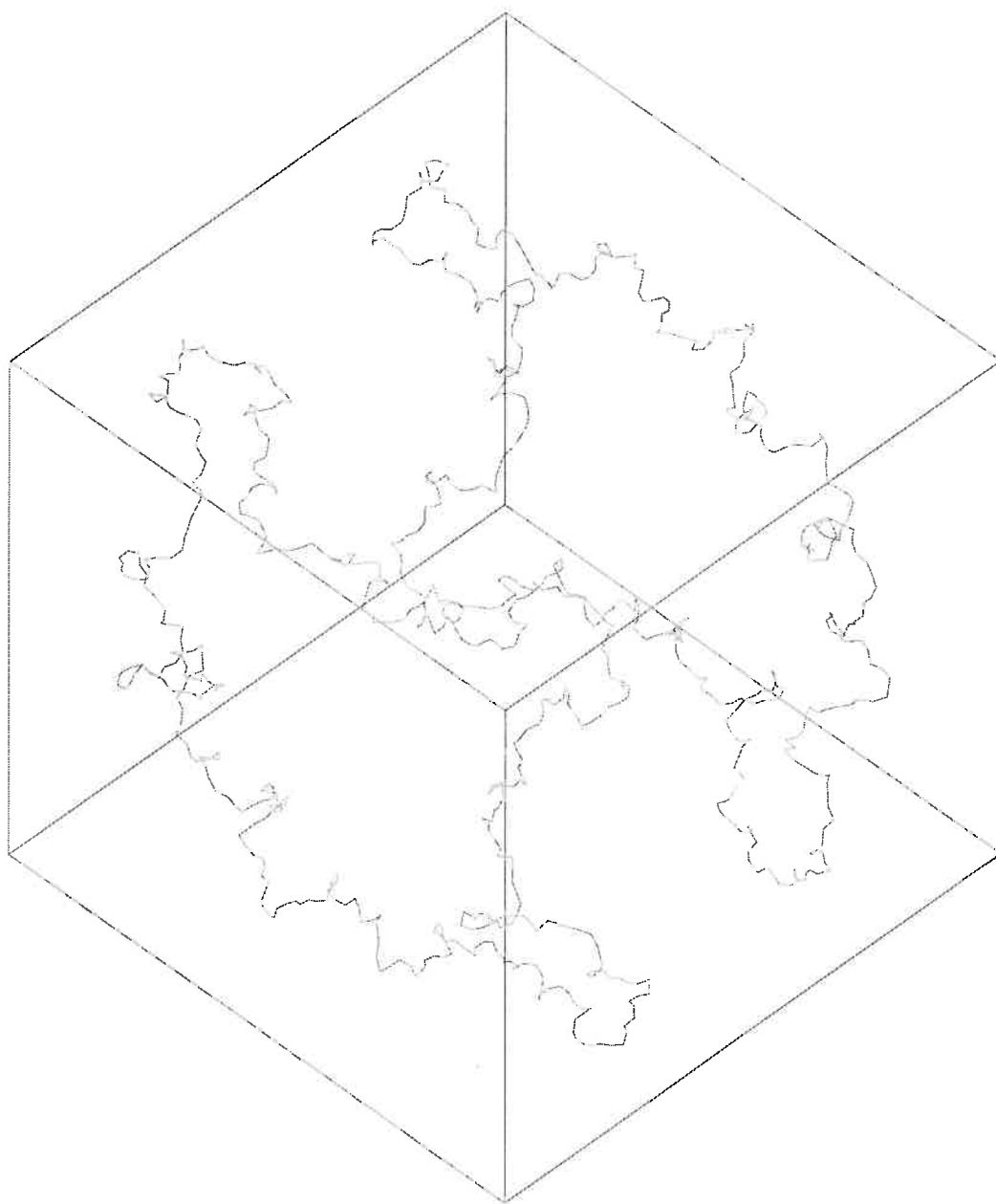
$t=0.059$

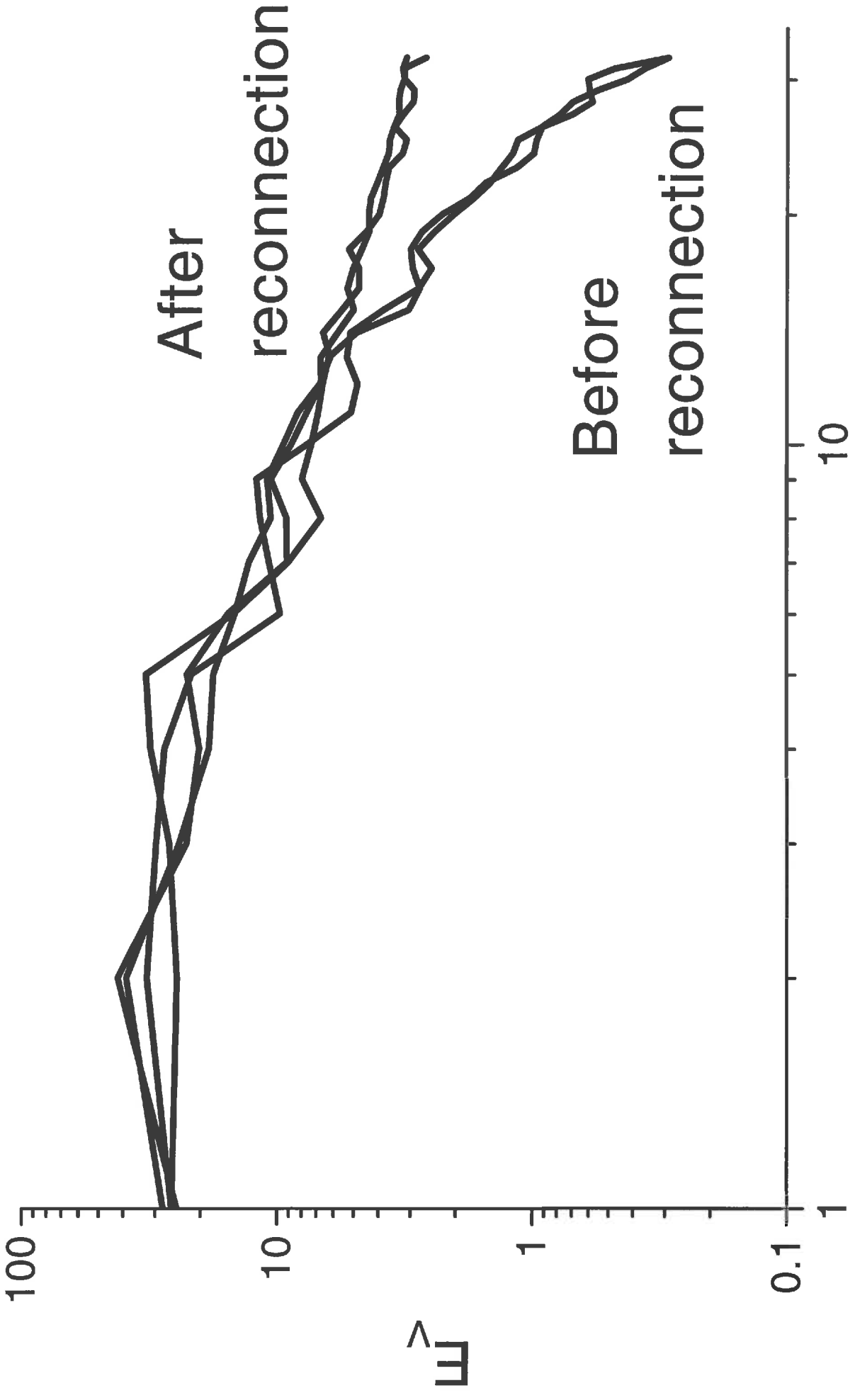


$t=0.069$



$t=0.129$





After

reconnection

Before

reconnection

10

K

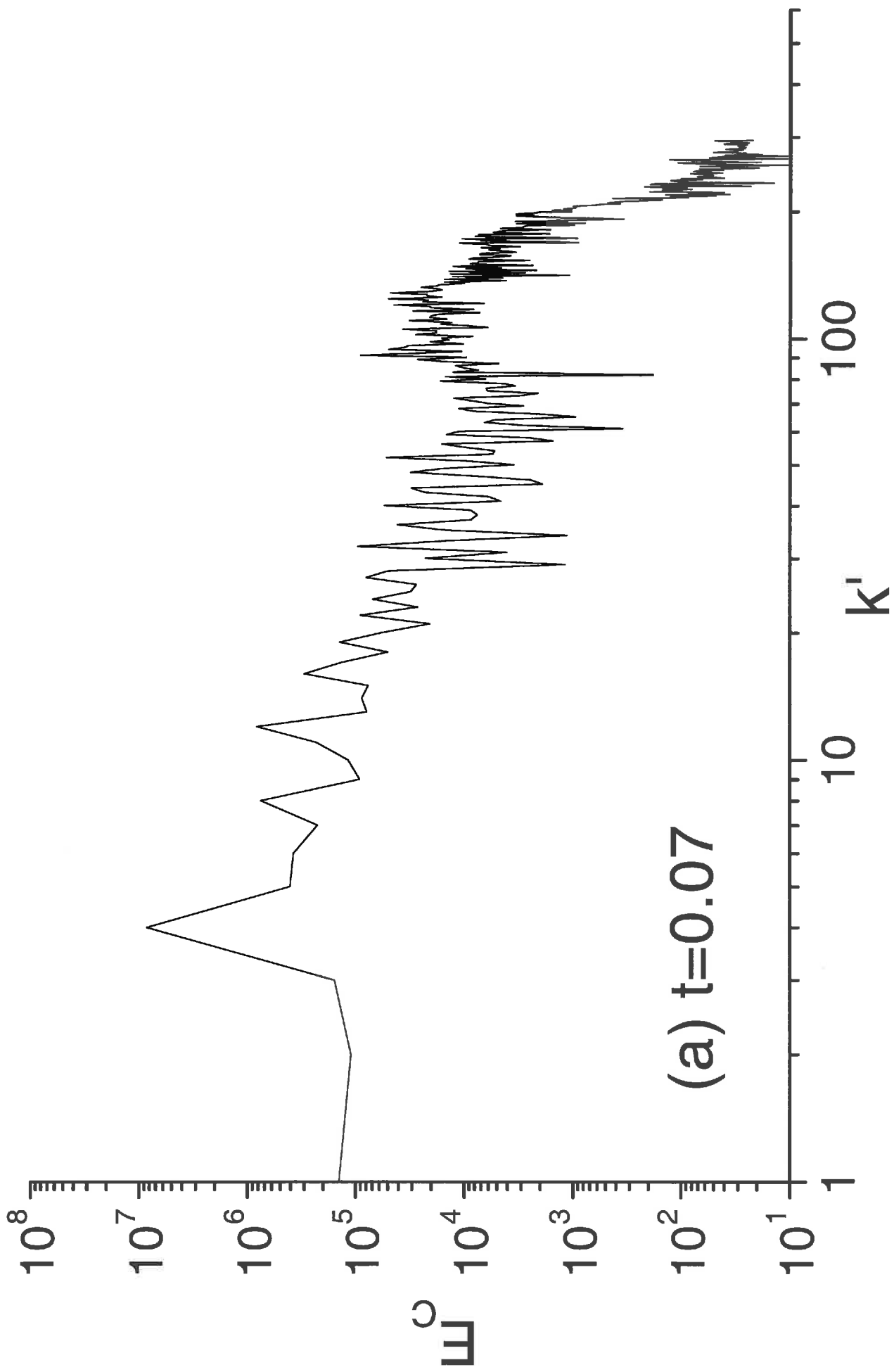
100

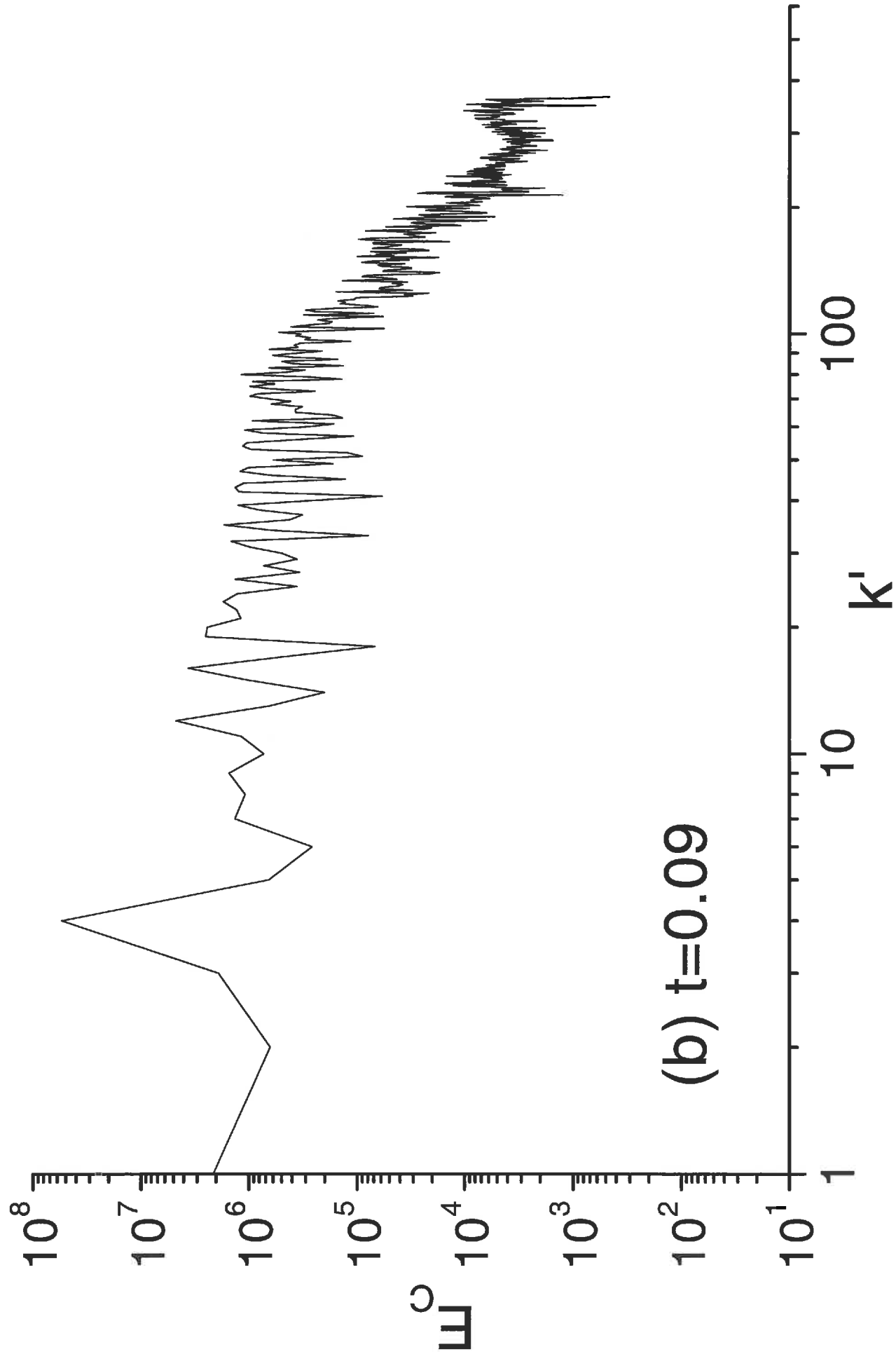
10

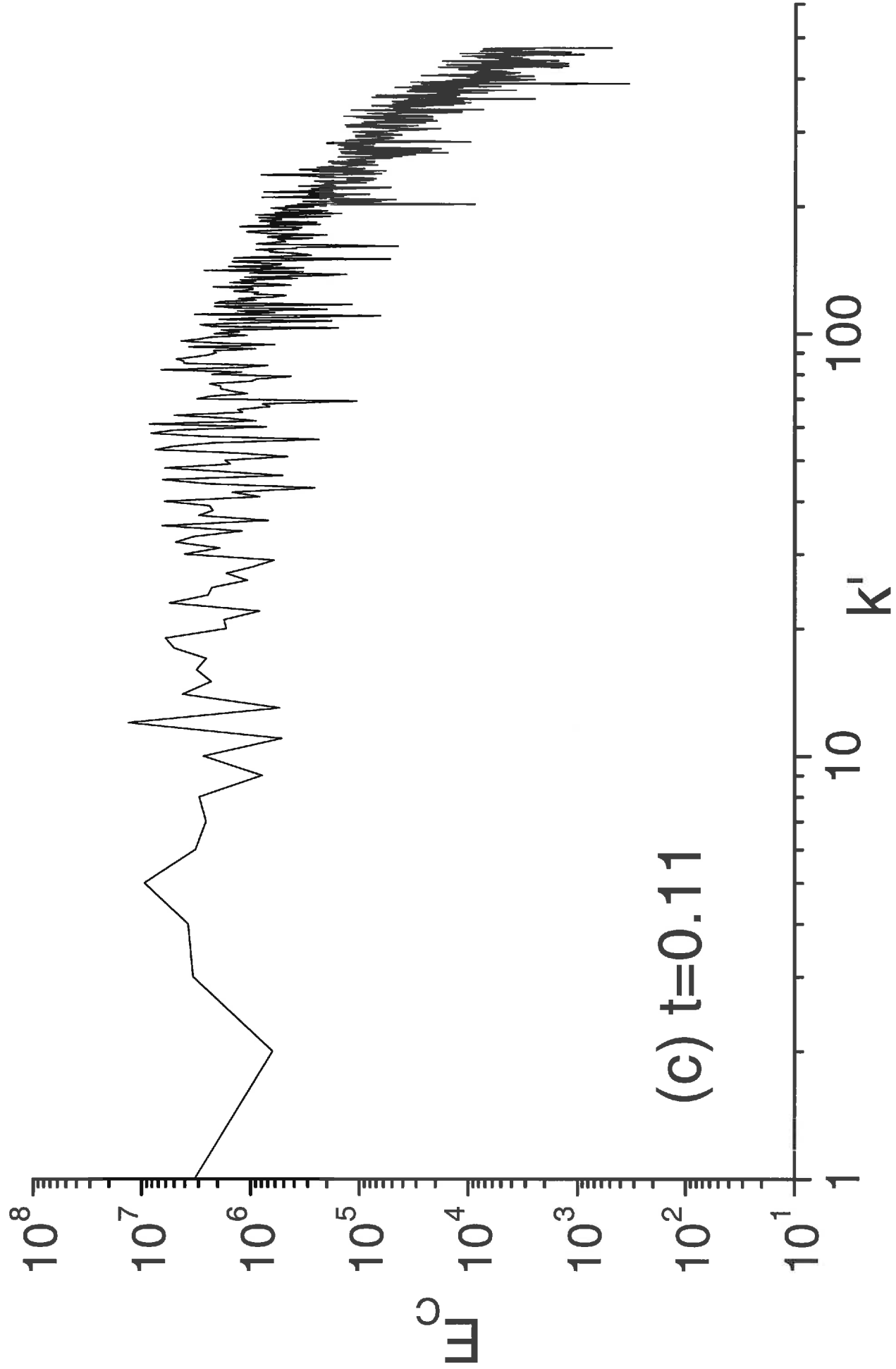
W^2

1

0.1







(c) $t=0.11$

